Table S1. Agreement of high confidence predicted contacts from residue co-evolution with PpdD pilus model, related to Figure 3. The accuracy (number of contacts with Prob > 0.7 consistent with the model/total number of contacts) is reported for increasing distance thresholds and for different rotameric states of the PpdD pilus model. A contact is considered as consistent with the model if the shortest distance between any non-hydrogen atoms of the two involved residues is smaller than the threshold. Optimized side-chain rotamers were built with SCWRL4.0 (Krivov et al., 2009). Alternatively, the at-most 10 best (most frequent) rotameric states from the Dunbrack library (Shapovalov and Dunbrack, 2011) were considered simultaneously to measure inter-residue distances in the PpdD pilus model.

Distance threshold (Å)	**PpdD pilus model (PDB 6GV9)**	**PpdD pilus model + optimized side-chain rotamers**	**PpdD pilus model + 10 best side-chain rotamers**
5	46.8 %	47.5 %	60.3 %
8	79.4 %	79.4 %	83.0 %
10	88.7 %	89.4 %	90.1 %
12	91.5 %	92.9 %	94.3 %

Table S2. Sequence and structure similarity between EHEC PpdD and other T4a pilins, related to Figure 1.

Pilin*	PDB id	% identity (full-length)	% identity (from Pro 22)	RMSD (Å)#
Ft PilE	3SOJ	25	16	2.7
Pa K122-4 PilA	1QVE	31	23	2.8
Pa PAK PilA	1OQW	30	22	2.8
Dn FimA	3SOK	28	20	3.0
Pa 110594 PilA	3JYZ	26	18	3.1
Ab PilA	5IHJ	30	20	3.1
Nm PilE	5JW8	32	26	3.2
Ng PilE	1AY2	32	26	3.2

* Ft : *Francisella tularensis* ; PaK122-4 : *Pseudomonas aeruginosa* strain K122-4 ; PAK : *Pseudomonas aeruginosa* strain PAK ; Dn : *Dichelobacter nodosus* ; Pa110594 : *Pseudomonas aeruginosa* strain Pa110594 ; Ab : *Acinetobacter baumannii* ; Nm : *Neisseria meningitidis* ; Ng : *Neisseria gonorrhoeae*.
# Computed with TM-align (Zhang and Skolnick, 2005).

Table S3. Plasmids used in this study, related to STAR Methods.

Plasmid name	Ori/resistance[1]	Relevant markers	Source/reference
pCHAP8184	ColE1/Ap^R	*pulS,pulAB pulCDEFHIJKLMNO*	(Campos *et al.*, 2010)
pSU18	p15A/Cm^R	*placZ-lacZα*	(Bartolome et al., 1991)
pUC18	ColE1/Ap^R	*placZ-lacZα*	(Yanisch-Perron et al., 1985)
pCHAP8565	p15A/Cm^R	*ppdD EHEC*	(Luna Rico et al., 2019)
pCHAP6263	p15A/Cm^R	*ppdD^{E5A}*	This study
pCHAP6250	p15A/Cm^R	*ppdD^{D35R}*	This study
pCHAP6254	p15A/Cm^R	*ppdD^{R29E}*	This study
pCHAP6256	p15A/Cm^R	*ppdD^{E131K}*	This study
pCHAP6257	p15A/Cm^R	*ppdD^{E92K}*	This study
pCHAP6258	p15A/Cm^R	*ppdD^{K83E}*	This study
pCHAP6260	p15A/Cm^R	*ppdD^{R74D}*	This study
pCHAP6261	p15A/Cm^R	*ppdD^{K30E}*	This study
pCHAP6264	p15A/Cm^R	*ppdD^{R44D}*	This study
pCHAP6265	p15A/Cm^R	*ppdD^{D106R}*	This study
pCHAP6266	p15A/Cm^R	*ppdD^{R116D}*	This study
pCHAP6267	p15A/Cm^R	*ppdD^{D132R}*	This study
pCHAP6268	p15A/Cm^R	*ppdD^{E48K}*	This study
pCHAP6269	p15A/Cm^R	*ppdD^{E53K}*	This study
pCHAP6317	p15A/Cm^R	*ppdD^{D58K}*	This study
pCHAP6271	p15A/Cm^R	*ppdD^{D61R}*	This study
pCHAP6272	p15A/Cm^R	*ppdD^{D123R}*	This study
pCHAP6316	p15A/Cm^R	*ppdD^{D35K}*	This study
pCHAP6320	p15A/Cm^R	*ppdD^{K30D}*	This study
pCHAP6333	p15A/Cm^R	*ppdD^{R74E}*	This study
pCHAP6319	p15A/Cm^R	*ppdD^{D106K}*	This study
pCHAP6321	p15A/Cm^R	*ppdD^{R29D}*	This study
pCHAP6253	p15A/Cm^R	*ppdD^{D137K}*	This study
pCHAP6262	p15A/Cm^R	*ppdD^{D138R}*	This study
pCHAP6280	p15A/Cm^R	*ppdD$^{D137K\ D138R}$*	This study
pCHAP6259	p15A/Cm^R	*ppdD^{R135E}*	This study
pCHAP6327	p15A/Cm^R	*ppdD$^{D35K\ R74D}$*	This study
pCHAP6337	p15A/Cm^R	*ppdD$^{D35K\ R74E}$*	This study
pCHAP8968	p15A/Cm^R	*ppdD$^{D35R\ R74D}$*	This study
pCHAP8969	p15A/Cm^R	*ppdD$^{D137R\ D138K\ R74D}$*	This study
pCHAP8970	p15A/Cm^R	*ppdD$^{D137R\ D138K\ R74E}$*	This study
pCHAP6314	p15A/Cm^R	*ppdD^{E92R}*	This study
pCHAP6257	p15A/Cm^R	*ppdD^{E92K}*	This study
pCHAP6259	p15A/Cm^R	*ppdD^{R135E}*	This study
pCHAP6322	p15A/Cm^R	*ppdD^{R135D}*	This study
pCHAP6277	p15A/Cm^R	*ppdD$^{E92K\ R135E}$*	This study
pCHAP6285	p15A/Cm^R	*ppdD$^{E92K\ R135D}$*	This study
pCHAP8956	p15A/Cm^R	*ppdD$^{D35K\ R135E}$*	This study
pUT18c	ColE1/Ap^R	*placUV5-cyaA* T18 fragment in pUC18	(Karimova et al., 1998)
pKT25	p15A/Km^R	*placUV5-cyaA* T25 fragment in pSU38	(Karimova et al., 1998)
pCHAP8501	ColE1/Ap^R	*T18-ppdD*	(Luna Rico et al., 2019)
pCHAP8504	p15A/Km^R	*T25-ppdD*	(Luna Rico et al., 2019)
pCHAP8973	ColE1/Ap^R	*T18-ppdD^{E5A}*	This study
pCHAP8768	ColE1/Ap^R	*T18-ppdD^{R29E}*	This study
pCHAP8770	ColE1/Ap^R	*T18-ppdD^{K30E}*	This study
pCHAP8772	ColE1/Ap^R	*T18-ppdD^{D35K}*	This study
pCHAP8774	ColE1/Ap^R	*T18-ppdD^{R44D}*	This study
pCHAP8776	ColE1/Ap^R	*T18-ppdD^{E48K}*	This study
pCHAP8916	ColE1/Ap^R	*T18-ppdD^{D58K}*	This study
pCHAP8780	ColE1/Ap^R	*T18-ppdD^{D61K}*	This study

pCHAP8782	ColE1/Ap^R	*T18-ppdD^{R74D}*	This study
pCHAP8784	ColE1/Ap^R	*T18-ppdD^{R116D}*	This study
pCHAP8786	ColE1/Ap^R	*T18-ppdD^{R135E}*	This study
pCHAP8920	ColE1/Ap^R	*T18-ppdD^{K83E}*	This study
pCHAP8922	ColE1/Ap^R	*T18-ppdD^{E92K}*	This study
pCHAP8924	ColE1/Ap^R	*T18-ppdD^{D106R}*	This study
pCHAP8926	ColE1/Ap^R	*T18-ppdD^{D123R}*	This study
pCHAP8928	ColE1/Ap^R	*T18-ppdD^{E131R}*	This study
pCHAP8930	ColE1/Ap^R	*T18-ppdD^{D132R}*	This study
pCHAP8936	ColE1/Ap^R	*T18-ppdD^{D138R}*	This study
pCHAP8155	p15A/Km^R	*T25-pulM*	(Nivaskumar et al., 2016)
pCHAP8910	p15A/Km^R	*T25-hofN*	(Luna Rico et al., 2019)
pMS41	ColE1/Ap^R	EHEC T4PS (*ΔppdD, hofBC, hofMNOPQ, ppdAB- ygdB-ppdC, gspO)*	(Luna Rico et al., 2019)

[1]ori, replication origin group, Ap^R, ampicillin-resistance; Cm^R, chloramphenicol-resistance, Km^R, kanamycin-resistance).

Table S4. Oligonucleotides used in this study, related to STAR Methods.

Oligonucleotide name	Sequence (5'-3')
PpdD-SD-EcoRI	CTATTCGAATTCAAAGTAGCGCCAACCAAATC
PpdD-Hind-3	cacAAGCTTGCATGCCTGCAGGTCGACTCTAG
HofC EcoRI 5	CACGAATTCGAAGAGTTAATCCGCGTATTG
HofC Hind 3	GACTGCAAGCTTCGTTATCCCATCCCACTCATCG
HofM Pst 5	CGCCTGCAGGGTAGTATAAAGGCAAGC
HofQ Sph 3	CACGCATGCCACGTTCAGCGTAAAAAC
PpdD 5 Kpn	GCAGGTACCTATGACACTTATCGAACTGATGGTG
PpdD 3 Eco	CACGAATTCCATTTCAGTGAGCTGTGGAAT
PpdDE5A 5 Kpn	GCAGGTACCTATGACACTTATCGcACTGATGGTG
PpdD D35R 5	CAAAGCCGCACTCACCcgCATGCTACAAAC
PpdD D35R 3	GTTTGTAGCATGcgGGTGAGTGCGGCTTTG
PpdD E5A 5	GTTTTACACTTATCGcACTGATGGTGG
PpdD E5A 3	CCACCATCAGTgCGATAAGTGTAAAAC
PpdD R29E 5	CAAAACTACCTGgaaAAAGCCGCACTC
PpdD R29E 3	GAGTGCGGCTTTttcCAGGTAGTTTTG
PpdD R29D 5	TATCAAAACTACCTGgaCAAAGCCGCACTCACC
PpdD R29D 3	GGTGAGTGCGGCTTTGtcCAGGTAGTTTTGATA
PpdD K30E 5	ACTACCTGCGCgAAGCCGCACTC
PpdD K30E 3	GAGTGCGGCTTcGCGCAGGTAGT
PpdD K30D 5	CAAAACTACCTGCGCgAtGCCGCACTCACCGAC
PpdD K30D 3	GTCGGTGAGTGCGGCaTcGCGCAGGTAGTTTTG
PpdD R44D 5	CCTTTGTGCCTTACgaTACCGCCGTAGAG
PpdD R44D 3	CTCTACGGCGGTAtcGTAAGGCACAAAGG
PpdD K30D 5	CAAAACTACCTGCGCgAtGCCGCACTCACCGAC
PpdD K30D 3	GTCGGTGAGTGCGGCaTcGCGCAGGTAGTTTTG
PpdD D35K 5	AAAGCCGCACTCACCaAaATGCTACAAACCTTTG
PpdD D35K 3	CAAAGGTTTGTAGCATtTtGGTGAGTGCGGCTTT
PpdD R74D 5	CCTACCACCACCgaCTATGTTTCAGCC
PpdD R74D 3	GGCTGAAACATAGtcGGTGGTGGTAGG
PpdD R74E 5	CCCTCGCCTACCACCACCgaaTATGTTTCAGCCATGAGTG
PpdD R74E 3	CACTCATGGCTGAAACATAttcGGTGGTGGTAGGCGAGGG
PpdD D106R 5	CATGACGCCAGGTTGGcgTAACGCAAACGGCGTCAC
PpdD D106R 3	GTGACGCCGTTTGCGTTAcgCCAACCTGGCGTCATG
PpdD D106K 5	ATGACGCCAGGTTGGaAaAACGCAAACGGCGTC
PpdD D106K 3	GACGCCGTTTGCGTTtTtCCAACCTGGCGTCAT
PpdD D137K 5	GTCTTCCGCTTTaAaGACGCCAACTAAG
PpdD D137K 3	CTTAGTTGGCGTCtTtAAAGCGGAAGAC
PpdD D138R 5	GTCTTCCGCTTTGATcgCGCCAACTAAGG
PpdD D138R 3	CCTTAGTTGGCGcgATCAAAGCGGAAGAC
PpdD D137K D138R 5	AAGATGTCTTCCGCTTTaAacgcGCCAACTAAGGAGC
PpdD D137K D138R 3	GCTCCTTAGTTGGCgcgtTtAAAGCGGAAGACATCTT
PpdD E131K 5	CAGCAAGCCTGCaAAGATGTCTTCC
PpdD E131K 3	GGAAGACATCTTtGCAGGCTTGCTG
PpdD E92K 5	CTGACCGGGCAAaAgAGTCTCAATGG
PpdD E92K 3	CCATTGAGACTcTtTTGCCCGGTCAG
PpdD K83E 5	CATGAGTGTGGCAgAGGGCGTGGTG
PpdD K83E 3	CACCACGCCCTcTGCCACACTCATG

PpdD D132R 5	GCAAGCCTGCGAACGTGTCTTCCGCTTTGATGACG
PpdD D132R 3	CGTCATCAAAGCGGAAGACACGTTCGCAGGCTTGC
PpdD D123R 5	GCAATATTCAAAGTCGCAGCGCATTGCAGC
PpdD D123R 3	GCTGCAATGCGCTGCGACTTTGAATATTGC
PpdD D61R 5	GGATTAGATACCTGCCGCGGTGGCAGCAATGG
PpdD D61R 3	CCATTGCTGCCACCGCGGCAGGTATCTAATCC
PpdD R135E 5	GAAGATGTCTTCgaATTcGATGACGCCAAC
PpdD R135E 3	GTTGGCGTCATCgAATtcGAAGACATCTTC
PpdD E48K 5	CCTTACCGTACCGCCGTAAAGTTGTGCGCGCTGG
PpdD E48K 3	CCAGCGCGCACAACTTTACGGCGGTACGGTAAGG
PpdD E53K 5	GGTATCTAATCCACCATGTTTCAGCGCGCACAACTCTACG
PpdD E53K 3	GCCACCGTCGCAGGTtTtTAATCCACCATGTTC
PpdD D58K 5	GAACATGGTGGATTAaAaACCTGCGACGGTGGC
PpdD D58K 3	CCACCGTCGCAGGTACGTAATCCACCATGTTCC
PpdD R116D 5	CGTCACCGGCTGGGCGgaCAACTGCAATATTCAAAG
PpdD R116D 3	CTTTGAATATTGCAGTTGtcCGCCCAGCCGGTGACG
PpdD R44E E48K 5	CCTTACgaaACCGCCGTAaAGTTGTGCGCGCTGG
PpdD R44E E48K 3	CCAGCGCGCACAACTtTACGGCGGTttcGTAAGG
PpdD R44D E48R 5	GCCTTACgaTACCGCCGTAcgtTTGTGCGCGCTGGAACATG
PpdD R44D E48R 3	CATGTTCCAGCGCGCACAAacgTACGGCGGTAtcGTAAGGC

Table S5. Refinement statistics of the PpdD pilus structure, related to STAR Methods.

Deviation from ideal geometry	
RMS[a] for bond lengths	0.02 Å
RMS for bond angles	2.40 °
Cβ deviations	0 %
Molprobity statistics	
Ramachandran favoured	92.0 %
Ramachandran allowed	6.5 %
Ramachandran outliers	1.4 %
Rotamer outliers	0 %
Clashscore	28.7
Overall score	2.43

[a] RMS, root mean square

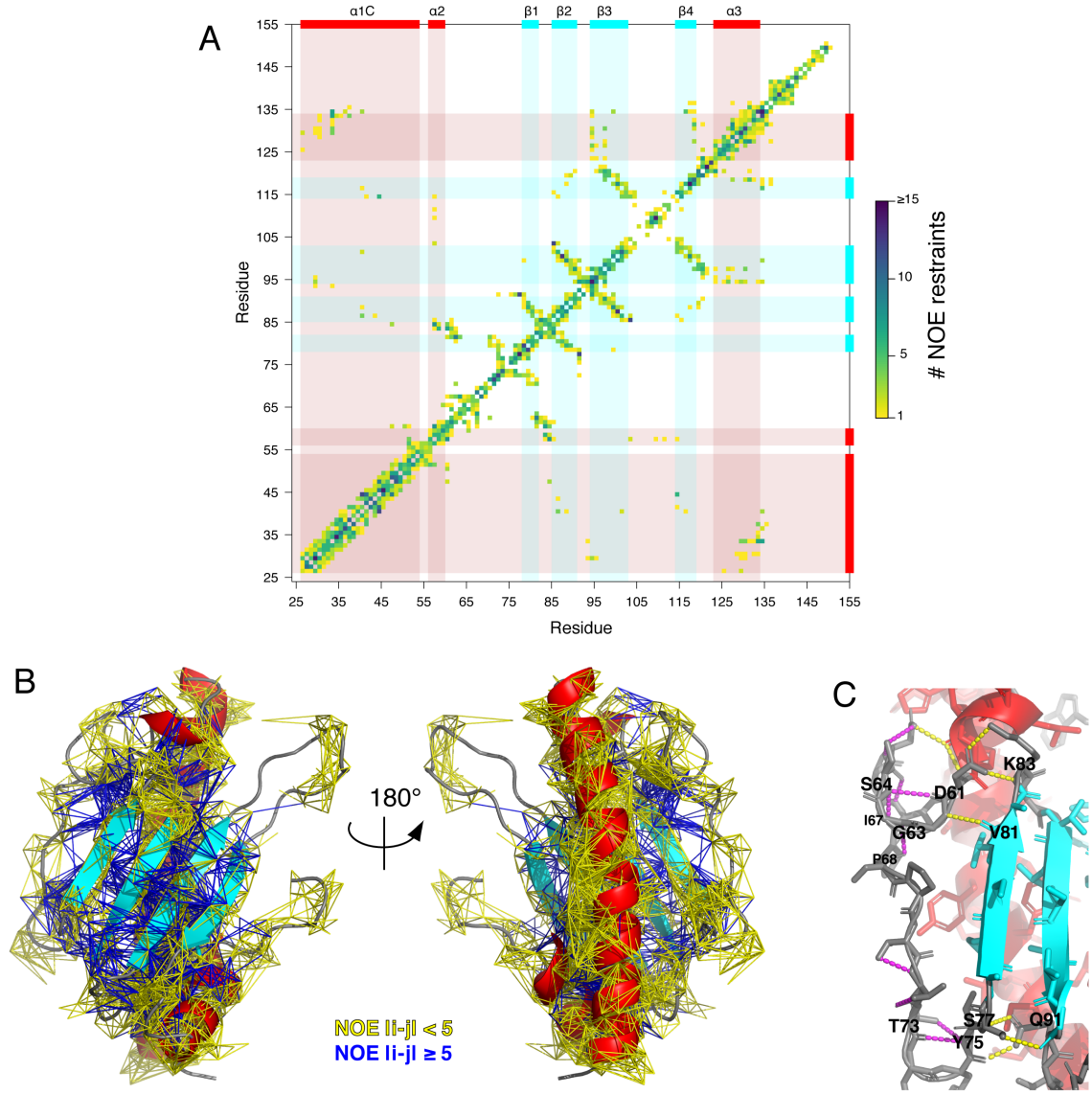

Figure S1. NOE restraints of the PpdDp NMR structure, related to Table 1. (A) Map of inter-residue NOE restraints used to calculate the PpdDp structure. The color scale corresponds to the number of unique NOE restraints for a pair of residues. Secondary structures are shown in red (helix) and cyan (strands). (B) NOE restraints shown on the lowest energy conformer of the PpdDp NMR structure. Long range NOE restraints are shown with blue lines and other NOE restraints with yellow lines. (C) Hydrogen-bonds detected in the PpdDp structure stabilizing the α/β loop.

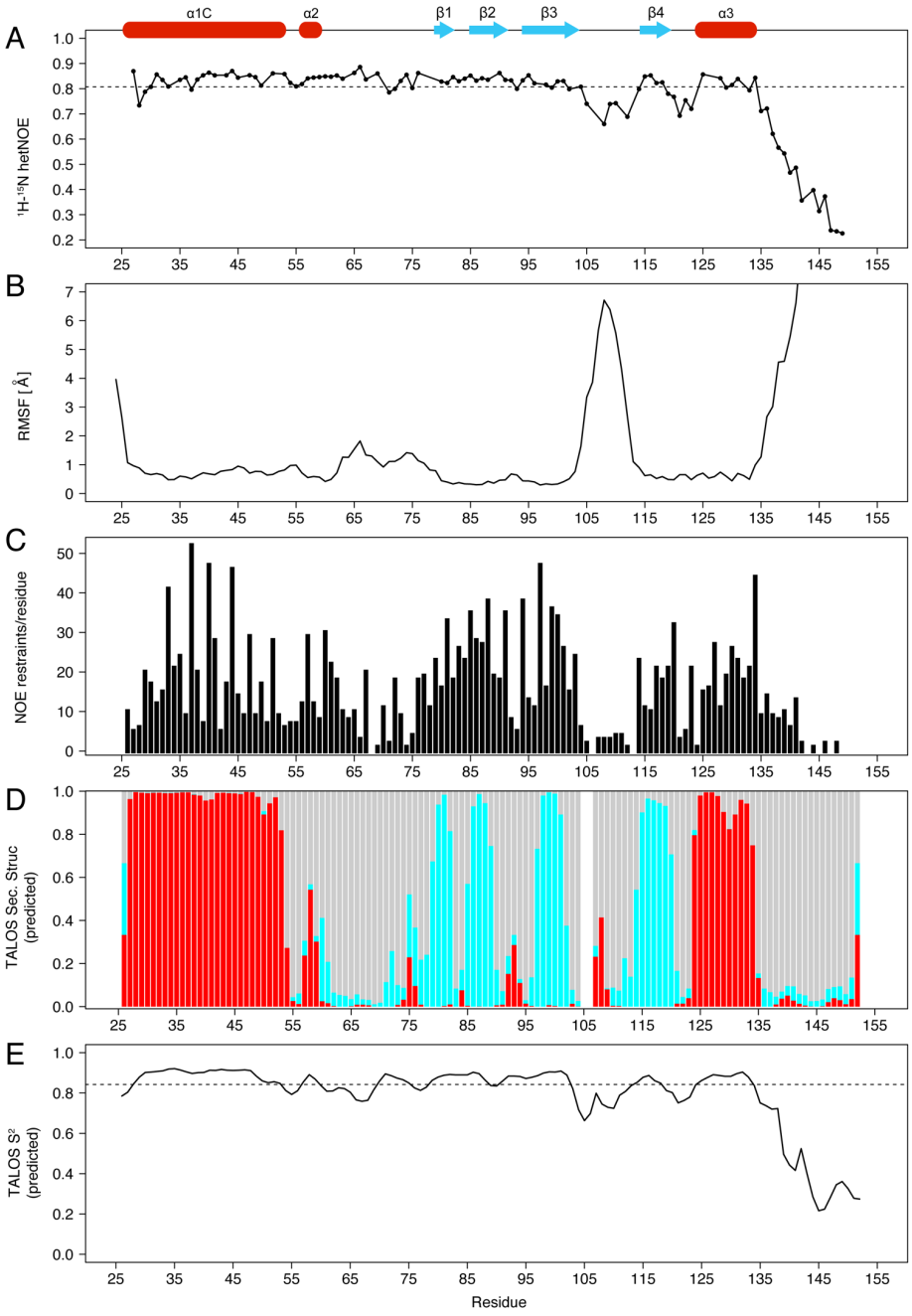

Figure S2. Dynamics and flexibility of PpdDp in solution, related to Figure 1. (A) ^{1}H-^{15}N heteronuclear NOE of PpdDp in solution. Secondary structure elements are shown on top (helix in red, strand in blue). (B) Ensemble Root Mean Square Fluctuation (RMSF) of the NMR PpdDp bundle. (C) Number of NOE (|i-j|> 1) restraints per residue as assigned by ARIA. (D) Secondary structure (probabilities) predicted from chemical shifts using TALOS+ (red: helix, cyan: strand, grey: loop). (E) TALOS+ predicted order parameter S^2.

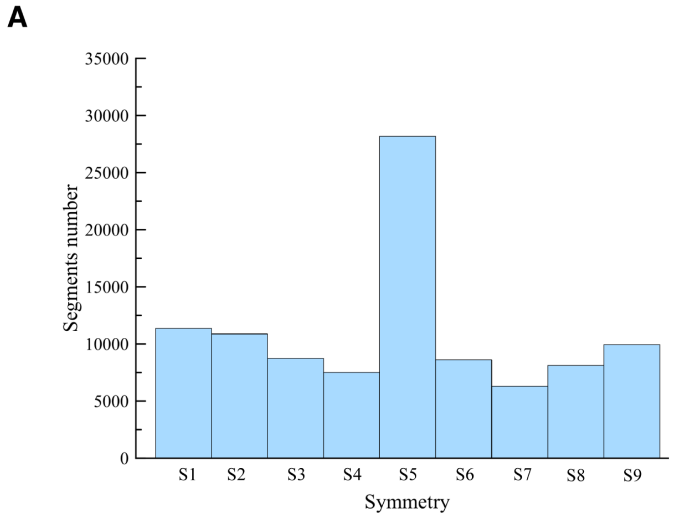

B

Symmetry	Twist	Rise
S1	94°	8.8Å
S2	96°	8.8Å
S3	98°	8.8Å
S4	94°	10.8Å
S5	96°	10.8Å
S6	98°	10.8Å
S7	94°	12.8Å
S8	96°	12.8Å
S9	98°	12.8Å

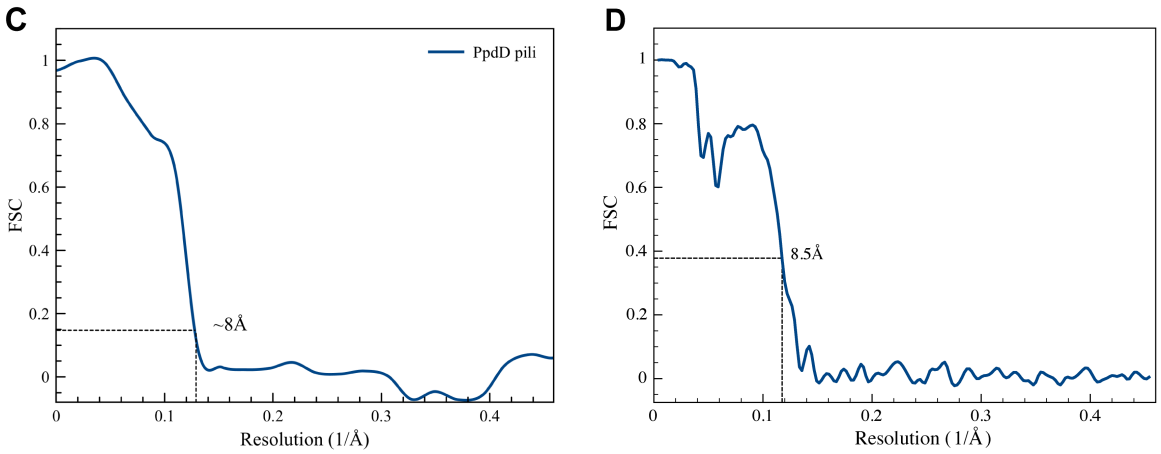

Figure S3. Large variability in terms of the helical symmetry of PpdD pili, related to Figure 2. (A) Histogram showing the symmetry distribution of PpdD pili segments. Nine reconstructions were generated with symmetry parameters shown in (B). These volumes were used for classifying the PpdD pili segments into different groups using a multi-reference alignment. (C, D) Fourier Shell Correlation (FSC) curves for the PpdD pili reconstruction. (C) The FSC of two half-maps shows a resolution of 8 Å at FSC=0.143. (D) The FSC curve for the refined PpdD pili model and the PpdD density map shows a resolution of 8.5 Å at FSC=0.38 (=√0.143).

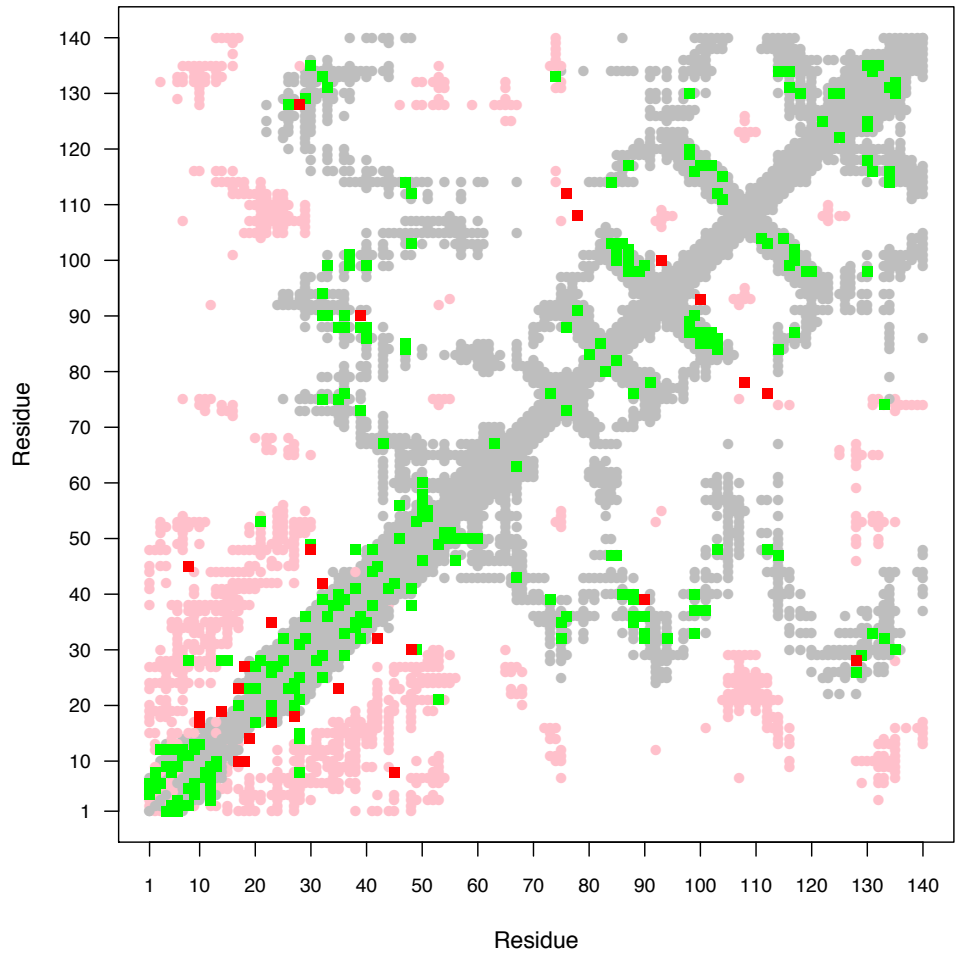

Figure S4. EHEC PpdD pilus contact map and evolutionary contact predictions, related to Figure 3. Inter-residue contacts in PpdD pilus ($d_{i,j}$ < 8 Å) are shown in grey (intra-protomer) and pink (inter-protomer). High confidence evolutionary contact predictions from Gremlin (Kamisetty et al., 2013) are shown in green (consistent with PpdD pilus model with $d_{i,j}$ < 10 Å) and red (inconsistent).

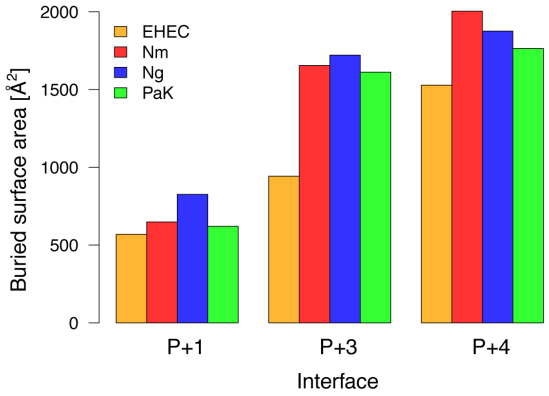

Figure S5. Buried surface areas of inter-subunit interfaces in T4Pa structures, related to Figure 6. Surface area was determined using atomic solvent accessible areas of isolated and complexed pilin subunits computed with the NACCESS program (Hubbard and Thornton, 1993).

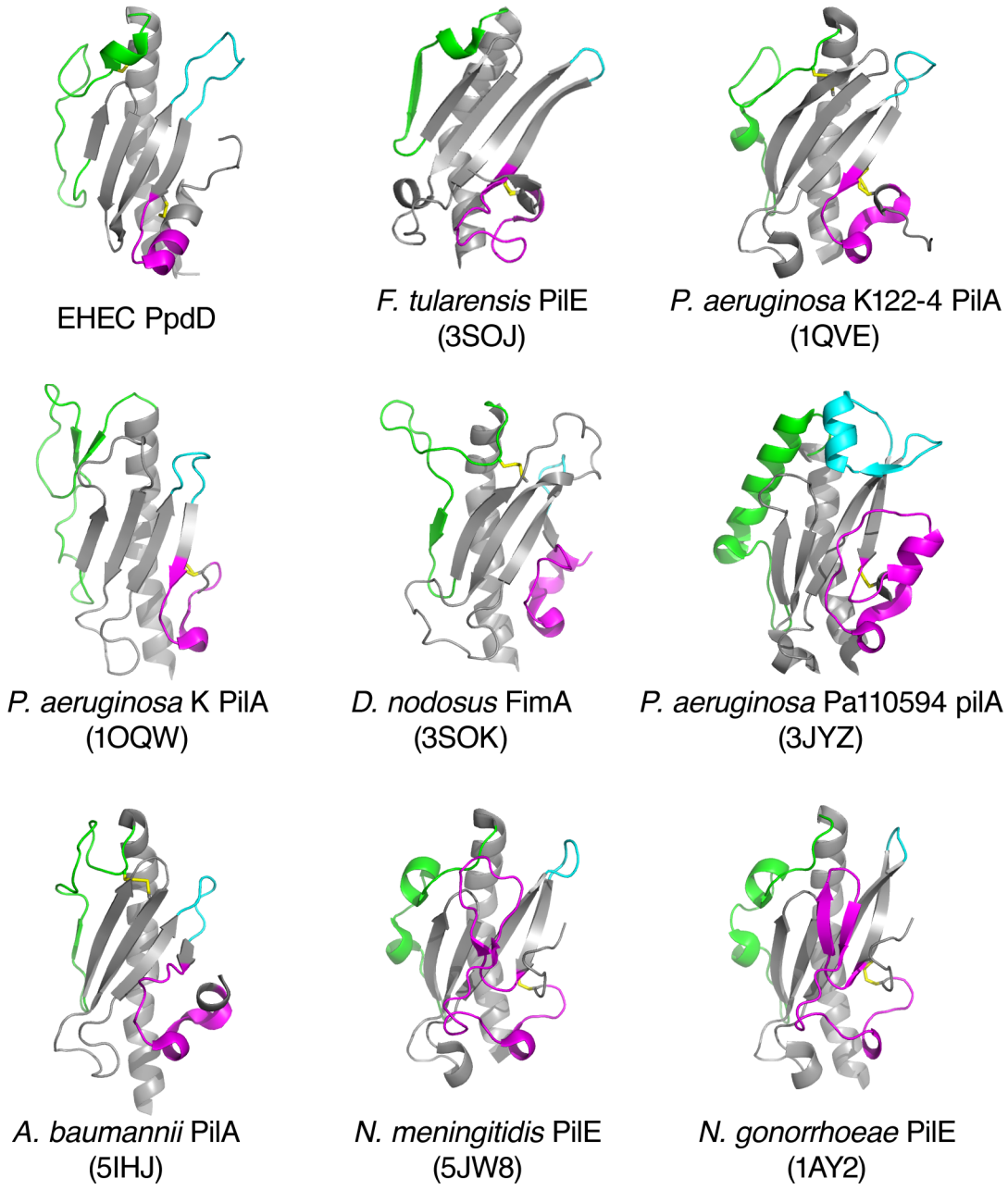

Figure S6. Structural comparison of major T4a pilins (periplasmic domains), related to Figure 1. α/β loop is shown in green, β3/ β4 loop in cyan and D-region in magenta.

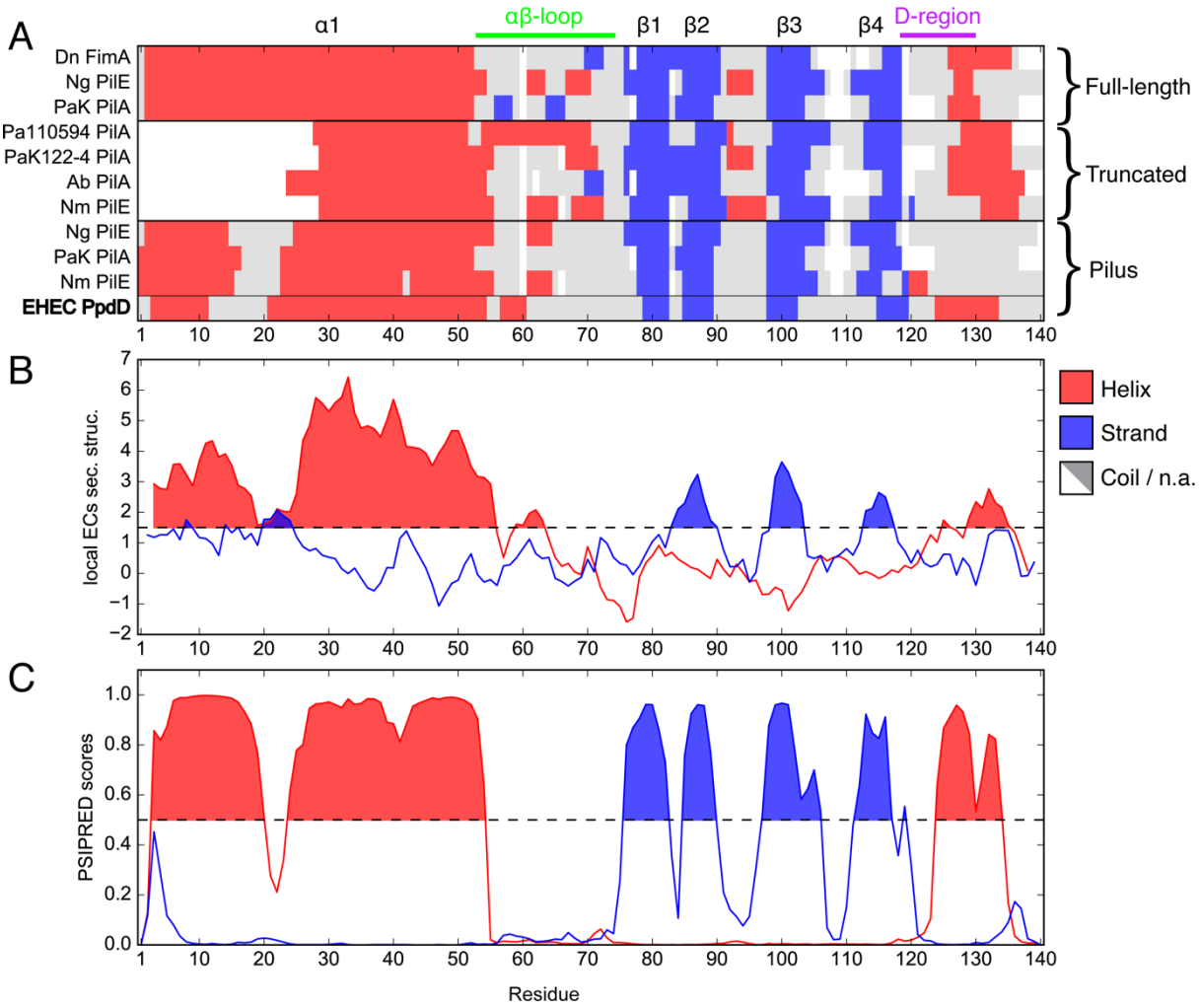

Figure S7. Secondary structure elements in T4a pilins, related to Figure 7. (A) Position of secondary structures elements of T4a pilin structures aligned on EHEC PpdD sequence and grouped according to the constructs and techniques used to solve the structure (Structures of full-length pilins solved by X-ray, truncated pilins missing the transmembrane segment and pilus structures solved by cryoEM). (B) Secondary structure score predicted from local evolutionary contacts within the T4a pilin family (Toth-Petroczy et al., 2016). (C) Secondary structure confidence score predicted with PSIPRED (Jones, 1999) on the EHEC PpdD pilin sequence.

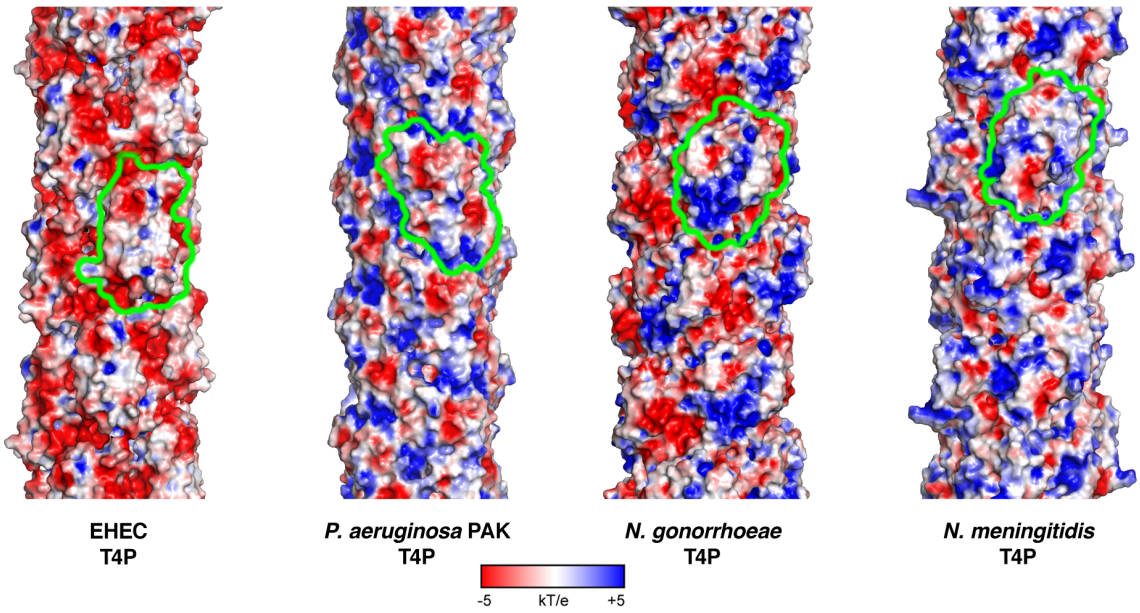

Figure S8. Surface electrostatics potential of T4P pilus structure, related to Figure 7. Electrostatics potential calculations were performed using APBS (Baker et al., 2001). The green lines delineate the surface of a single pilin subunit.